

國立交通大學

生物科技系

碩士論文

Phe427 在 *Arthrobacter globiformis* 組織胺氧化酵素

之受質特異性中的角色



**The Role of Phe427 on the Substrate Specificity of**

***Arthrobacter globiformis* Histamine Oxidase**

研究生：余震世

指導教授：袁俊傑 博士

中華民國九十九年一月

Phe427 在 *Arthrobacter globiformis* 組織胺氧化酵素  
之受質特異性中的角色

The Role of Phe427 on the Substrate Specificity of  
*Arthrobacter globiformis* Histamine Oxidase

研究生：余雯世

Student：Wen-Shih Yu

指導教授：袁俊傑 博士

Advisor：Dr. Chiun-Jye Yuan

國立交通大學

生物科技系



Submitted to Department of Biological Science and Technology

National Chiao Tung University

in partial Fulfillment of the Requirements

for the Degree of

Master

in

Biological Science and Technology

January 2010

Hsinchu, Taiwan, Republic of China

中華民國九十九年一月

# Phe427 在 *Arthrobacter globiformis* 組織胺氧化酵素

## 之受質特異性中的角色

學生：余雯世

指導教授：袁俊傑博士

國立交通大學生物科技系暨研究所碩士班

### 中文摘要

含銅胺類氧化酵素 (Copper-containing amine oxidase, CAO)

[EC1.4.3.6]廣泛存在於各種生物之中。該類酵素催化一級胺類的氧化脫胺作用且在各種不同生物有多元化的功能，如提供細菌生長所需的碳源及氮源、參與植物細胞防禦等機制，在動物中亦參與許多代謝機制。不同生物來源的含銅胺類氧化酵素對胺類受質特異性差別很大。*Arthrobacter globiformis*之組織胺氧化酵素（簡稱AGHO）屬於CAO的一種，為了了解哪些胺基酸決定AGHO的受質特異性，我們利用針對不同物種之CAO之間的序列比對及分子模擬方法選定了AGHO胺基酸序列中的Ala156、Pro157、Leu158及Phe427進行定點突變。兩套突變株分別模擬*Hansenula Polymorpha*的甲基胺氧化酵素(methylamine oxidase，簡稱HPAO)及動物中牛血清胺類氧化酵素(Bovine serum amine oxidase，簡稱BSAO) 其活性區的胺基酸序列。酵素經由大腸桿菌表現、純化及活化步驟之後，測定突變株對於原本偏好的受質胺類與模擬之物種的受質胺類的活性及特異性。研究結果顯示模擬HPAO的突變株對於特定碳鏈長度的芳香族胺類選擇性提高；而模擬BSAO的突變株對原本偏好的受質之特異性降低，並對BSAO的偏好受質之特異性及活性提高。本研究說明了Ala156、Pro157、Leu158及Phe427這四個胺基酸位置扮演了與受質特異性有關的角色，並且證明針對特定胺基酸的定點突變可以改變AGHO之受質特異性。

# **The Role of Phe427 on the Substrate Specificity of**

## ***Arthrobacter globiformis* Histamine Oxidase**

Student : Wen-Shih Yu

Advisor : Dr. Chiun-Jye Yuan

Department of Biological Science and Technology

National Chiao Tung University

### **Abstract**

Copper-containing amine oxidase (CAO) catalyzes the oxidative deamination of primary amines, and they are ubiquitous in nature and have diverse biological functions ranging from bacteria to mammals. CAOs from different sources possess various substrate preferences. *Arthrobacter globiformis* histamine oxidase (AGHO) is a member of the CAO family. To understand what residues in the active site determine the substrate specificity of AGHO, multiple sequences alignment and molecular modeling between different sources of CAOs were performed to pick four potential residues Ala156, Pro157, Leu158 and Phe427 for site-directed mutagenesis. Two sets of AGHO mutants were generated with one set mimics the active site residues of *Hansenula Polymorpha* methylamine oxidase (HMAO), while the other set mimics the active site residues of *Bovine* serum amine oxidase (BSAO). These mutants and the wild type AGHO were bacterial expressed, purified and subjected to activity and kinetics studies. In the report, the mutants mimicking HMAO altered the substrate specificity to aromatic amines with different chain lengths. Whereas, the mutants mimicking BSAO showed decreased specificities to histamine but exhibited a higher catalytic activity to typical substrates for BSAO. It is suggested that the Ala156, Pro157, Leu158 and Phe427 play important roles in the substrate recognition and selection. And the substrate specificity of AGHO could be modified or altered through site-directed mutagenesis.

# Contents

中文摘要 .....	i
Abstract .....	ii
Contents .....	iii
Figure Contents .....	v
Table Contents .....	vi
Appendix Contents .....	vii
Introduction .....	1
Materials and Methods .....	9
Vector and Expression System .....	9
Reagents .....	9
Construction of Expression Plasmids .....	9
Site-Directed Mutagenesis .....	10
E. coli Expression of Recombinant AGHO <sup>WT</sup> and AGHO <sup>mutants</sup> .....	11
Purification of Recombinant AGHO <sup>WT</sup> and AGHO <sup>mutants</sup> .....	11
Reconstitution of Recombinant AGHO <sup>WT</sup> and AGHO <sup>mutants</sup> .....	12
Protein Concentration Determination .....	13
Oxidation Activity Assay .....	13
H <sub>2</sub> O <sub>2</sub> Standard Curve .....	14
Kinetic Measurement .....	14
Electrophoresis and Redox-Cycling Staining .....	15
Result and Discussion .....	17
1. The Construction of Mutants of AGHO and Expression of Wild Type and Mutants of AGHO .....	17
2. Biogenesis of TPQ in AGHO Mutants .....	17
3. Study of Substrate Preference of Wild Type AGHO .....	18
4. Studies of Substrate Preference of Mutants AGHO .....	20

4-1. Selection of Residues in AGHO for Site-Directed Mutagenesis	20
4-2. A156D, F427N and A156D/F427N mutants	21
4-2-1. Relative activities of A156D, F427N and A156D/F427N mutants with various substrates	21
4-2-2. Kinetic studies of A156D, F427N and A156D/F427N mutants with various substrates	22
4-3. A156S/P157G and L158D mutants	23
4-3-1. Relative activities of A156S/P157G, and L158D mutants with various substrates	23
4-3-2. Kinetic studies of A156S/P157G and L158D mutant with various substrates	24
4-4. A156S/P157G/L158D, F427S and A156S/P157G/L158D/F427S mutants	26
4-4-1. Relative activities of A156S/P157G/L158D, F427S and A156S/P157G/L158D/F427S mutants with various substrates	26
4-4-2. Kinetic studies of A156S/P157G/L158D, F427S and A156S/P157G/L158D/F427S mutants with various substrates	27
5. Conclusion	28
6. Future Application of AGHO	28
Reference	30

## Figure Contents

Figure 1. The H <sub>2</sub> O <sub>2</sub> standard curve was determined within the range from 0.1 to 15 nmole of H <sub>2</sub> O <sub>2</sub> .....	34
Figure 2. 10% SDS-PAGE of crude extract and purified protein of wild type AGHO and its mutants.....	35
Figure 3. 10% SDS-PAGE of purified of wild type AGHO and its mutants.....	36
Figure 4. NBT/glycinate staining of the wild type AGHO and the its mutants.....	37
Figure 5. Plots of relative activities toward various amines between wild type AGHO and A156D, F427N and 156D/F427N.....	38
Figure 6. The proposed model for the binding of spermine in the active site of A156S/P157G/L158D.....	39
Figure 7. The proposed model for the binding of spermine in the active site of A156, P157, L158 and F427.....	40

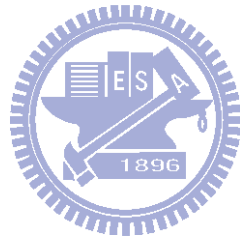
## Table Contents

Table 1. CAOs are known to vary a great deal in their preferred substrate specificities.....	41
Table 2. Relative activities of wild type AGHO reacted with various substrates.....	42
Table 3. $K_m$ , $K_{cat}$ , $K_i$ and $K_{cat} / K_m$ values toward various substrates of wild type AGHO.....	43
Table 5. The multiple sequences alignment of CAOs on the selected residues involved in substrate binding.....	45
Table 6. Relative activities of A156D, F427N and A156D/F427N mutants of AGHO reacted with various substrates.....	46
Table 7. $K_m$ , $K_{cat}$ , $K_i$ and $K_{cat} / K_m$ values toward various substrates of A156D (A), F427N (B) and A156D/F427N (C) mutants of AGHO .....	47
Table 8. Relative activities of L158D and A156S/P157G mutants of AGHO reacted with various substrates.....	49
Table 9. $K_m$ , $K_{cat}$ , $K_i$ and $K_{cat} / K_m$ values toward various substrates of L158D (A) and A156S/P157G (B) mutants of AGHO .....	50
Table 10. Relative activities of A156S/P157G/L158D, F427S and A156S/P157G/L158D/F427S mutants of AGHO reacted with various substrates.....	51
Table 11. $K_m$ , $K_{cat}$ , $K_i$ and $K_{cat} / K_m$ values toward various substrates of A156S/P157G/L158D (A), F427S (B) and A156S/P157G/L158D/F427S (C) mutants of AGHO.....	52



## Appendix Contents

Appendix 1. Plasmid map of pET30b(-S)/AGHO .....	54
Appendix 2. List of amines .....	55
Appendix 3. List of plasmids and vectors .....	57
Appendix 4. List of primers for site-directed mutagenesis.....	58
Appendix 5. Abbreviations of CAOs from different source .....	59



## Introduction

Amine oxidases are broadly divided into two groups based on their cofactors, flavin-dependent monoamine oxidases (MAOs) and quinone-containing copper amine oxidases (CAOs). Copper amine oxidase (CAO) catalyzes the oxidative deamination of primary amines to the corresponding aldehyde and ammonia coupled with the reduction of oxygen to hydrogen peroxide. CAOs are ubiquitous in nature and have proposed biological functions that are as diverse as the myriad of host organisms in which the enzyme is found [1]. CAOs have been found in many different organisms ranging from bacteria to mammals. They are the most widespread family of quinone-proteins, and can be found in practically every kingdom of life with the exception of the archaea [2].

In bacteria, the CAOs have a well-defined role in the metabolism of primary amines as alternate sources of carbon and nitrogen to support growth. In plants, the production of hydrogen peroxide ( $H_2O_2$ ) deriving from polyamine oxidation has been correlated with cell wall maturation and lignification during development as well as with wound-healing and cell wall reinforcement during pathogen invasion. As a signal molecule,  $H_2O_2$  derived from polyamine oxidation mediates cell death, the hypersensitive response and the expression of defence genes. Furthermore, aminoaldehydes and 1,3-diaminopropane from polyamine oxidation are involved in secondary metabolite synthesis and abiotic

stress tolerance [3]. In mammals, CAOs has been proposed to play a role in the metabolism of glucose and the trafficking of leukocytes, being implicated in diseases such as diabetes and atherosclerosis, they have been implicated as key components in complex processes such as leukocyte trafficking involving the CAO, vascular adhesion protein-1 (VAP-1) [4].

CAOs are classified into different types based on the active site cofactors. Among the well-known quinocofactors, topa quinone (TPQ) is ubiquitous, existing in both prokaryotic and eukaryotic enzymes that include a divergent class of CAOs. Besides the lack of the TPQ consensus sequence and its reduced size, the most fundamental difference lies in its unique cofactor structure. Lysine tyrosylquinone (LTQ) recently has been identified as the active site cofactor in mammalian lysyl oxidase by isolation and characterization of a derivatized active site peptide [5].

The catalytic cycle of CAOs has been demonstrated. The key structures are the Cu atom, the cofactor topa quinone (TPQ), and the active-site base, for instance, the aspartate residue. The first step in catalysis is Schiff-base formation at C(5) of the TPQ and followed by proton abstraction and hydrolysis with the aldehyde product released. And then the reduced, NH<sub>2</sub>-substituted TPQ is reoxidized by oxygen via a Cu(I)-semiquinone intermediate. Finally TPQ is regenerated by hydrolysis with releasing of ammonia [6].

CAOs are generally composed of two identical subunits with a molecular weight ranging from 70 to 100 kDa. Each monomer contains a copper and an

organic cofactor, TPQ, post-translationally derived from a tyrosine residue. The formation of the quinone has been shown to be a self-processing event requiring both copper and molecular oxygen. One important feature of CAOs is the presence of both a metal ion and a protein-derived cofactor in close proximity. In most cases, the metal ion is copper that provides a potentially redox active ion, and the cofactor is TPQ [2]. Currently, the crystal structures of several CAOs have been determined, ECAO (*Escherichia coli* amine oxidase; PDB code: 1OAC [7]), AGPEO (*Arthrobacter globiformis* phenylethylamine oxidase; PDB code: 1AV4 [8]), HPAO (*Hansenula polymorpha* amine oxidase; PDB code: 1A2V [9]), PSAO (CAOs from *Pisum sativum*; PDB code: 1KSI [6]), BSAO (CAOs from bovine plasma; PDB code: 1TU5 [10]), hVAP-1 (human vascular adhesion protein; PDB code: 1US1 [11]), and PPLO (lysyl oxidase from *Pichia pastoris*; PDB code: 1N9E [12]). These CAOs share a similar 3D structure, though they actually exhibit a low amino acid sequences identity of 25~35%.

Each subunit of the dimer is composed of three domains, usually labeled D2-D4 [10]. The N-terminal domain D2 is the smallest, and a long stretch connects domain D2-D3. Domain D3 and D4 are connected by a long stretch, too. Domain D4, located at the C-terminal, is the largest and comprises about 400 residues. It represents the core of the CAO molecule and includes the active-site. D4 is structurally the most conserved domain among different amine oxidases. Domains D2 and D3 of each subunit are located at the opposite side with respect to the molecule 2-fold axis and they do not interact in the dimer;

nevertheless, the two D4 domains present a large contact area.

The active site of CAOs, located between two sheets of  $\beta$ -sandwich, has two distinct components: cofactor TPQ and the Cu(II) ion. The Cu(II) is coordinated by three His residues, conserved in all the CAO sequences, from bacteria to eukaryotes: two of them lie on the same strand, while the third is close to the C-terminus. TPQ is located at the bottom of a big and funnel-shaped cavity located in a region of the molecule surface near the junction of domains D3 and D4 [8]. The opening of the cavity of one subunit is partially occupied by the end of a hairpin structure of the other subunit. And it may play a role in substrate recognition. This arm exhibits a low amino acid homology among CAOs from different species. Differences in amino acid composition in this region provide unique characteristics to a given CAO in terms of the electrostatic properties, dimensions of the substrate channel, and the accessibility of substrates to TPQ.

In [8], they reported a channel in AGAO, which seems to be suitable for the movement of reactants and reaction products to and from the active site. The molecular surface surrounding the entrance to the channel is predominately negatively charged. Since amine substrates are recognized in the protonated, positively charged form. The charges being associated with the side chains of Glu102, Glu103, Glu106 and Glu109 of domain D3 and Asp 357 on arm I from domain D4 of the other subunit of the dimer. The electrostatic potential and surface topology at the entrance to the channel are thought to be important for substrate recognition. The internal surface of the channel is lined by residues

which become more hydrophobic as they approach the active site. At the end of the channel is the side chain of Tyr296 which acts as a “gate” to the active site. The side chain of Tyr permits unhindered access to the active site. The key to the recognition of the channel (in AGAO) is the absence of electron density corresponding to the phenol ring of Tyr 296. Similar channel was found to exist in PSAO [13] and ECAO [14], though the channel in PSAO crystals is narrower than in AGAO, and the channel in ECAO crystals is partly obstructed (Phe298 in PSAO; Tyr381 in ECAO). The above shows that the channel provides the required access of the substrate to the active site.

The substrate preference of recombinant AGHO was studied by Yang [15] and Chen [16] in our laboratory. The recombinant AGHO exhibits a substrate preference not only to histamine but also to other aromatic amines, such as phenylethylamine and tyramine. The active site pocket of AGHO is surrounded by hydrophobic amino acid residues, suggesting that AGHO prefers hydrophobic substrates. The  $K_{cat}/K_m$  value of AGHO to various substrates also increased with the raising hydrophobicity of amines. And the  $K_m$  value decreased in nearly a linear fashion with increasing chain length of the alkyl carbon chain of aromatic amines. The kinetics study on site-directed mutated AGHO carried out by Chen reveals that three conjugated residues (A156, P157 and L158) which are positioned on the entrance to the channel play important roles in controlling the substrate specificity. And the replacement of these three amino acid residues may alter the substrate specificity of AGHO. The

CAOs from different species exhibit diverse substrate specificities (Table 1) [17]. Chen generated one set of mutants, A156D and A156D/L158W, which mimic the tripeptide sequence of HPAO (*Hansenula Polymorpha* amine oxidase) and another set of mutants, L158D, A156S/P157G and A156S/P157G/L158D, which mimic the tripeptide sequence of BSAO (*Bovine* serum amine oxidase). The AGHO mutant A156S/P157G/L158D exhibits an obviously high catalytic activity to physiological polyamines, which are typical substrates for BSAO. BSAO prefers aliphatic amines, including putrescine, spermine, and spermidine, as its substrates [18, 19, 20].

In Chang's study [21], a novel QSAR (quantitative structure activity relationships) model for AGHO was developed. The model can probe the relationship between affinities of AGHO and hydrophobicities of ligands. The correlative residues were compressed into F126, A156, P157, L158, Y316, D318, Y322, V399, N401 and F427 through the QSAR model and sequence alignment between the CAOs from different species. In Chen's study [16], the residues A156, P157 and L158 were selected to be site-directed mutated. And it was expected the site-directed mutation would alter the substrate specificities of AGHO. The kinetics study of the recombinant wild type and site-directed-mutated AGHO were carried out. In the results, A156D, which mimics *Hansenula Polymorpha* methylamine oxidase (HPAO, a CAO of Kingdom Fungi), shows alternated activities to various representative amines. And A156S/P157G/L158D, which mimics *Bovine* serum amine oxidase (BSAO

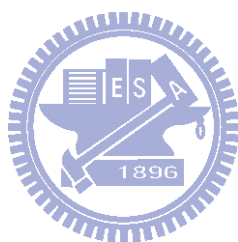
a CAO of kingdom animalia, exhibits an extremely high catalytic activity to physiological polyamines, which are typical substrates for BSAO.

The amino acid sequence of the tripeptide (156-158) is highly homologous in CAOs from species within a kingdom since it is less conserved across different kingdoms (table 4, table 5). This tripeptide may play an important role in substrate recognition, structure stability, and enzyme activity. In Chen's study [16], the reactivity of the wide type AGHO to spermine (compared with the activity of the wild type AGHO to histamine) is 0.2%, and the reactivity of the A156S/P157G/L158D mutant to spermine is 6.1%, which is 30 times more reactive than the wild type AGHO. At the same time, the  $K_{cat}$  values of the A156S/P157G/L158D mutant to aromatic amines are reduced when the  $K_m$  values are similar to the wild type AGHO. Compared with the wild type AGHO, the  $K_{cat}/K_m$  values of the A156S/P157G/L158D mutant to aromatic amines are reduced 5 to 11 folds.

In Chen's study [16], the data suggests that A156 and L158 of AGHO may play important roles in mediating the substrate selectivity and in controlling the binding and/or catalysis of substrates. A156 of AGHO may play a key role in mediating the catalysis of amines. L158 may be important in determining the substrate selectivity of CAOs. The residues A156, P157 and L158 of AGHO were studied in previous studies by Yang [15] and Chen [16], and in this study, we try to investigate the role of residue F427. Two groups of mutants of AGHO were generated. One group, which includes A156D, F427N and A156D/F427N,



is intended to mimic the amino acid sequence of HPAO. The other group, which includes A156S/P157G/L158D, L158D, A156S/P157G, F427S and A156S/P157G/L158D/F427S, is intended to mimic the amino acid sequence of BSAO. These mutants and the wild type AGHO are overexpressed, purified and activated. Then they were subjected to activity and kinetics study.



## Materials and Methods

### *Vector and Expression System*

Recombinant wild type AGHO and the mutants of AGHO genes were inserted into plasmid pET30b(-S) (Appendix 1)[27, 34, 35] and were transformed into *E. coli* BL21(DE3) cells.

### *Reagents*

The tested amines and chemicals were purchased from Merck™ and Sigma™. Spectra/Por molecularporous membrane for the dialysis procedure was obtained from Spectrum Medical Industries, Inc. The HisTrap-chelating columns for the purification of his-tagged proteins were purchased from GE Healthcare. Bradford's reagent for the determination of protein concentration was purchased from Bio-Rad. The DNA ladder and the protein molecular weight marker were purchased from MBI. The prestained protein ladder was purchased from Fermentas. The Polyvinylidene difluoride (PVDF) membrane was obtained from Millipore™. All restriction enzymes were purchased from New England Biolabs, Inc. *Puf*Turbo DNA polymerase was purchased from Merck. All reagents and chemicals that operated in the experiments were at reagent grade.

### *Construction of Expression Plasmids*

The wild type AGHO, A156D, A156D/L158W, A156S/P157G, L158D and

A156S/P157G/L158D mutants in pUC-T and the expression vector pET30(-S)/AGHO were constructed previously in our laboratory [15, 22, 23]. The NotI fragment of the wild type AGHO gene (2069 bp) was purified from the agarose gel and recovered with Gel/PCR DNA Fragments Extraction Kit (GENEAID). The NotI fragment of AGHO gene in pET30(-S)/AGHO was then replaced by the previously purified DNA fragment. The wild type AGHO in pGEM-T easy vector was constructed for the site-directed mutagenesis.

### ***Site-Directed Mutagenesis***

The A156D, A156D/L158W, A156S/P157G, L158D and A156S/P157G/L158D mutants of AGHO in pET30b (-S) were previously constructed in our laboratory. And F427N and F427S fragments were generated with QuickChange™ Site-Directed Mutagenesis protocol (STRATAGENE) with pGEM-T easy/AGHO as a template. The reaction reagents contained 50 ng DNA templates, 125 ng forward and reverse primers, 2.5 U *Puf*Turbo DNA polymerase, and 0.5 mM dNTP in a final volume of 50 µL. The PCR condition was set following the protocol of manufacturer. Then 10 U DpnI restriction enzyme was added into the resulting PCR product to remove the original methylated template. The product was then incubated at 37 °C overnight. The DpnI-treated PCR product (15 µL) was then transformed into DH5α competent cells and screened for mutants. Furthermore, the mutation sites were confirmed by DNA sequencing.

After the mutated sequences were confirmed, they were digested with SacI and NcoI restriction enzymes. The extracted F427S fragment (927 bp) was ligated into the SacI/NcoI site of wild type and A156S/P157G/L158D mutant in pET30b(-S). In the same way, the extracted F427N fragment was ligated into the cutting site of wild type AGHO and A156D mutant in pET30b(-S) instead.

### ***E. coli Expression of Recombinant AGHO<sup>WT</sup> and AGHO<sup>mutants</sup>***

The recombinant wild type AGHO and all the constructed mutants were overproduced in *E. coli* BL21(DE3) cells carrying plasmid pET30b(-S) with the wild type and mutated genes of AGHO. Single colonies picked from freshly streaked plates (LB-agar, supplemented with 25 µg/mL kanamycin) were incubated at 37 °C for 12 hours, and then inoculated into 200 mL of LB medium. Flask cultures were grown at 37 °C and shaken at a speed of 150 rpm until the cell density reached  $A_{600nm} = 0.4\sim 0.6$ . Cells were induced with 50 µM isopropyl-1-thio-β-D-galactopyranoside (IPTG) and cultivated at 25 °C for 8 hours. Cells were then harvested by centrifugation at 6,000 rpm for 30 minutes.

### ***Purification of Recombinant AGHO<sup>WT</sup> and AGHO<sup>mutants</sup>***

The cell pellets collected in the previous procedure were resuspended in 5 mL of buffer A (50 mM potassium phosphate buffer, pH 6.8) and then disrupted on ice by ultrasonic disintegration with the sonic dismembrator (550, Fisher Scientific). To remove insoluble particulates, the resulting lysates were then

centrifuged at 14,000 rpm for 30 minutes. The supernatants were first fractionated with ammonium sulfate (1-50%). The precipitates of 50% (w/w) ammonium sulfate were centrifuged at 10,000 rpm for 30 min and then dissolved in 1 mL of buffer A (50 mM potassium phosphate buffer, pH 6.8). The resuscitations were dialyzed against buffer A at 4 °C for 12 hours and the buffer was renewed every 4 hours.

A prepared HisTrap-chealating column (GE Healthcare) was set up for the purification of recombinant proteins. The protein solutions were applied to a 1 mL pre-packed column. The preparation was following the manufacturer's protocol. Briefly, the column was washed with 5 mL of distilled water prior to recharging Ni<sup>2+</sup> ions with 1 mL of 100 mM NiSO<sub>4</sub>. And then the column was washed with 1 mL distilled water to remove the unbound metal ions. After the preparation procedure, the column was equilibrated with 5 mL of binding buffer (20 mM Tris-HCl, pH 7.9, 500 mM NaCl, 5 mM imidazole). The protein solutions were centrifuged at 14,000 rpm for 15 min prior to the injection. After applying the sample onto the column, it was then washed with 10 mL of binding buffer. The column was washed with binding buffer containing 60 mM imidazole to remove the non-specifically bound proteins. The bound target proteins which are histidine-tagged were eluted with elution buffer (binding buffer with 500 mM imidazole) and were collected.

### ***Reconstitution of Recombinant AGHO<sup>WT</sup> and AGHO<sup>mutants</sup>***

The eluted proteins from previous purification were dialyzed overnight against buffer A with 50  $\mu\text{M}$   $\text{CuSO}_4$  to allow the TPQ formation and Cu(II) binding. The unbound or weakly bounded Cu(II) was removed by dialyzing with buffer A for at least three times of buffer changes, and each buffer change includes incubation at 4  $^\circ\text{C}$  for 4 hours .

### ***Protein Concentration Determination***

The concentration of purified AGHO was determined by Bradford protein assay (Bio-Rad). 800  $\mu\text{L}$  of ddH<sub>2</sub>O, 200  $\mu\text{L}$  Bradford reagent, and 2  $\mu\text{L}$  eluted protein solution were mixed. The mixture was applied to a vortex mixer and incubated under room temperature for 10 minutes. The absorbance of mixture at wavelength 595 nm on the glass cuvette on a spectrophotometer (Hitachi U-3010) was determined. The protein concentration was calculated through interpolation of the bovine serum albumin (BSA) standard curve plotted on the same machine.

### ***Oxidation Activity Assay***

Activity of amine oxidases (AGHO) was determined by monitoring the  $\text{H}_2\text{O}_2$  production of the reaction coupled to the oxidation of the chromogen, 3-dimethyl-aminobenzoic acid (DMAB), and the acceptor, 3-methyl-2-benzothiazolinone hydrazone (MBTH), by horseradish peroxidase (HRP) [24]. The coupled enzymatic reaction depends on the generation of  $\text{H}_2\text{O}_2$

by amine oxidases. In the presence of  $H_2O_2$  and peroxidase, the chromogen MBTH is oxidatively coupled to DMAB, forming a purple indamine dye with an adsorption maximum at 595 nm. Assays were carried out in 2 or 20  $\mu$ g enzyme reaction with amine substrate in the detection buffer (2.5 U horseradish peroxidase, 2 mM DMAB, and 0.04 mM MBTH in 50 mM sodium phosphate buffer, pH 7.4) in a total volume of 1 mL at 30 °C for 5 minutes. Absorbance measurement was obtained with Hitachi U-3010 using quartz cuvettes with 1 cm path length. The value of enzyme activity was calculated through the slope plotted of UV Solutions 2.1 on the same mechanism. A blank assay was carried out, in which the medium did not contain any substrate.



### ***H<sub>2</sub>O<sub>2</sub> Standard Curve***

The procedure is the same as that of activity assay except that amine oxidase and substrates were replaced with  $H_2O_2$  in amounts from 0.1 to 15 nmoles. The standard curve of  $H_2O_2$  concentration and the corresponding absorbance of 595 nm were illustrated in Figure 1.

### ***Kinetic Measurement***

The amine substrates used in this study were histamine, benzylamine, phenylethylamine, phenylpropylamine, phenylbutylamine, tyramine, methylamine, ethylamine, putrescine and spermine. All the amine substrate stock solutions were freshly prepared in distilled water. The choices of different

substrate concentrations of in the kinetic study varied due to the possibility of substrate inhibition effect. The oxidation of substrates was determination by previously described HRP-coupled assay, and all tests were repeated for three times. The data were fitted non-linearly by at least six substrate concentrations. The curve fitting was performed with Michaelis-Menten equation 1 on the SIGMA plot program Enzyme Kinetics Module 1.1.

$$V=V_{\max} / (1+K_m/[S]) \quad \dots\dots\dots\text{Equation 1}$$

And the substrates demonstrating substrate inhibition were performed with equation 2,

$$V=V_{\max} / (1+K_m/[S] +[S]/K_i) \quad \dots\dots\dots\text{Equation 2}$$



***Electrophoresis and Redox-Cycling Staining***

The extracted protein persevered in solutions were resolved by a 10% SDS polyacrylamide electrophoresis gel (SDS-PAGE). All SDS-PAGE procedures were performed with a Bio-Rad Mini Protein II apparatus. Protein samples were boiled for 5 min in the presence of 100 mM dithiothreitol before loading onto the loading wells of SDS-PAGE. The electrophoresis was performed at 100 volt for 20 minutes first, followed at 140 Volt for another 1.5 hours. After electrophoresis, the gel was stained with 0.1% Coomassie Blue. And the purities of purified protein samples were analyzed and calculated with the software ImageJ which was developed at the National Institutes of Health.

The redox-cycling approach provides a tool to reliably determine the



quinone content of proteins for the study of the biological significance of this process and the factors that affect protein quinolation. The redox-cycling staining with NBT-Glycinate was determined as previous described [25]. The proteins were separated on 10% SDS-polyacryamide gels and transferred to a polyvinylidene difluoroide (PVDF) membrane on a Bio-Rad Mini Trans-Blot Electrophoretic Transfer Cell soaked in an ice-cold transfer buffer (25 mM Tris, pH 8.3, 192 mM Glycine, 20% (v/v) methanol) at a constant current of 200 mA for 2 hours. After electro-blotting, the membrane was immersed in the Glycinate/NBT solution (0.24 mM Nitroblue Tetratzolium in 2 M potassium glycine, pH 10) for 30-45 minutes in the dark. The quinoproteins would be stained as blue-purple bands on the Membrane.



## Result and Discussion

### 1. The Construction of Mutants of AGHO and Expression of Wild Type and Mutants of AGHO

A156D, F427N, A156D/F427N, A156S/P157G, L158D, A156S/P157G/L158D, F427S, A156S/P157G/L158D/F427S mutants of AGHO were generated with QuickChange™ Site-Directed Mutagenesis in pGEM-T easy/AGHO template. Then the wild type and mutants of AGHO were expressed with the pET-based bacterial expression system of *E. coli*. These proteins were cultivated in a copper-depleted medium and purified to homogeneity following the protocol described by Yang in our laboratory [15]. As shown in figure 2 and figure 3, the purity of wild type and mutants of AGHO was >99% as verified by SDS-PAGE.

### 2. Biogenesis of TPQ in AGHO Mutants

In previous studies, we had demonstrated that in AGHO, the conversion of the precursor tyrosine into TPQ could be done in the presence of 50  $\mu\text{M}$   $\text{CuSO}_4$  [15]. To reduce the oxidative damage that Cu(II) do to the expressed recombinant AGHO, it was purified as an apo-form and would be activated prior the activity and kinetic study. After incubation with 50  $\mu\text{M}$   $\text{CuSO}_4$  for overnight, the purified AGHO may exhibit a pale pink color suggesting the formation of TPQ; whereas the untreated, inactive enzyme (presumably an apo-form) is

colorless. To verify the formation of TPQ in the recombinant AGHO after  $\text{Cu}^{2+}$  treatment, the redox-cycling staining was employed. TPQ has been shown to catalyze redox cycling under an alkaline pH with excess glycine as a reducing agent. In the presence of nitroblue tetrazolium and oxygen, tetrazolium is reduced to formazan and deposited onto the nitrocellulose membrane that contains recombinant AGHO.

The result (figure 4) ensures that the TPQ is formed in either the wide type AGHO or the mutants following the treatment of  $\text{Cu}^{2+}$ , indicating that the formation of TPQ in these mutants is unaltered by the mutagenesis. After the treatment, the unbound Cu(II) is removed by dialysis to ensure the maintenance of enzyme activity, and the activated enzymes are ready for further experiments.



### **3. Study of Substrate Preference of Wild Type AGHO**

Histamine is reported to be the primary substrate for AGHO, but other amines, including phenylethylamine, dopamine, aromatic monoamines, and aliphatic mono- and diamines are also suggested to be catalyzed by AGHO [26]. Therefore, the reactivity of active AGHO to various, natural, or xenobiotic amines (**Appendix 2**) were studied. Table 2 shows the relative activities of AGHO to various amines at the concentration of 0.2 mM. Compared with histamine (100%), the relative activities were calculated. The wild type AGHO exhibited higher activities to phenylethylamine ( $145.6 \pm 3.6\%$ ) and tyramine ( $112.7 \pm 3.2\%$ ). And it exhibited moderate activities to phenylpropylamine ( $38.1$

$\pm 1.9\%$ ) and phenylbutylamine ( $54.2 \pm 1.3\%$ ). AGHO shows very low activity to benzylamine ( $1.8 \pm 0.3\%$ ), putrescine ( $0.9 \pm 0.1\%$ ), and spermine ( $0.4 \pm 0.1\%$ ).

In table 3 kinetic constants ( $K_m$ ,  $K_{cat}$ ,  $K_{cat}/K_m$ ) of wild type AGHO to various amines are plotted and calculated by Michaelis-Menten equations. The initial reaction rate at each concentration of corresponding amine substrate was determined at 30°C within time duration from 0 to 300 seconds. The non-linear curve of initial rate (umol/min/mg) versus substrate concentration ( $\mu\text{M}$ ) was fitted by Michaelis-Menten equation 1. Equation 2 was used if the plot shows a substrate inhibition. Phenylethylamine, phenylpropylamine, phenylbutylamine and tyramine exhibit substrate inhibition to wild-type AGHO while the behavior is not observed in histamine and benzylamine. The reactivities of the wild type AGHO to putrescine and spermine were too low for the kinetic constants determination.

As shown in Table 3, the  $K_m$  value of wild type AGHO to aromatic amines including benzylamine ( $49.01 \pm 12.03 \mu\text{M}$ ), phenylethylamine ( $9.05 \pm 0.45 \mu\text{M}$ ), phenylpropylamine ( $7.50 \pm 0.97 \mu\text{M}$ ) and phenylbutylamine ( $2.23 \pm 0.60 \mu\text{M}$ ) decreased when the alkyl carbon chain that connects the aromatic ring and the amino group of the aromatic amines increases from 1 to 4 carbons. The  $K_m$  value of AGHO for tyramine ( $12.37 \pm 0.66 \mu\text{M}$ ), an amine with one hydroxyl group on the aromatic ring, is slightly higher than that of phenylethylamine ( $9.05 \pm 0.45 \mu\text{M}$ ). The values of  $k_{cat}/K_m$ , which represent the substrate specificity, are 0.0895, 0.0220,

0.8431, 0.2889, 1.2484, and 0.4606 ( $\mu\text{M}^{-1}\text{S}^{-1}$ ) for histamine, benzylamine, phenylethylamine, phenylpropylamine, phenylbutylamine, and tyramine, respectively. The result indicates that phenylethylamine and its derivatives are also preferred substrates for the wild type AGHO, and the AGHO reactivities towards these amines are even higher than it towards the original identified substrate, histamine.

#### **4. Studies of Substrate Preference of Mutants AGHO**

##### ***4-1. Selection of Residues in AGHO for Site-Directed Mutagenesis***

We have found that AGHO prefer hydrophobic amines as its substrates in our previous study [27]. The hydrophobicity of substrates is probably the determinant that affects the binding to AGHO, implying the presence of a lipophilic binding pocket at the active site of AGHO [8]. Thus, the hydrophobicity was set to be a crucial factor to build the QSAR model of AGHO [21]. Based on the built AGHO QSAR model, amino acids residues including F126, A156, P157, Y316, D318, Y322, V399, N401, and F427 were selected (Table 4). Most of the selected residues are non-polar except Y316, D317, Y322, and N400. The multiple sequences alignment of CAOs (Table 5) reveals that the residues Y316, D317, Y322, and N400 are either identical or highly conserved cross all five kingdoms. We discovered that residues A156, P157, L158 and F427 of AGHO are highly conserved within each kingdom; whereas the homology of these residues is low cross the kingdoms (Table 5). Hence, in this

study, several sets of single, double, triple and quadruple mutants of AGHO was generated to mimic the active site residues of a fungi amine oxidase, *Hansenula Polymorpha* amine oxidase (HPAO) (A156D, F427N, A156D/F427N), and an animal amine oxidase, bovine serum amine oxidase (BSAO) (L158D, F427S, A156S/P157G, A156S/P157G/L158D and A156S/P157G/L158D/F427S). Further kinetic studies were performed.

#### ***4-2. A156D, F427N and A156D/F427N mutants***

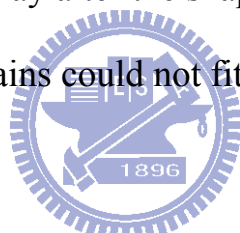
##### ***4-2-1. Relative activities of A156D, F427N and A156D/F427N mutants with various substrates***

In table 6, all the relative activities were compared to the activity of wild type AGHO toward histamine (100%). A156D exhibits lower relative activities to histamine (from 100.0% to 7.4%), benzylamine (from 1.8% to 0.8%), phenylethylamine (from 145.6% to 21.2%), phenylpropylamine (from 38.1% to 3.1%), phenylbutylamine (from 54.2% to 5.2%) and tyramine (from 112.7% to 14.6%). This set of mutants shows no reactivities to the HPAO substrates including methylamine and ethylamine. In the result, the mutation intends to mimic HPAO did not increase the reactivities to the preferred substrates of HPAO. F427N also shows lower relative activities to histamine (from 100.0% to 63.9%), benzylamine (from 1.8% to 1.5%), phenylethylamine (from 145.6% to 82.1%), phenylpropylamine (from 38.1% to 32.7%), phenylbutylamine (from 54.2% to 44.5%) and tyramine (from 112.7% to 73.5%), but mutation on F427

made a less obvious decrease than on A156 (figure 5). Both A156D and F427N show nearly no activity to putrescine and spermine.

Relative activities of A156D/F427N toward histamine, phenylethylamine and tyramine are 6.4 %, 12.8% and 9.4%, respectively. And it shows no detected activity to benzylamine, phenylpropylamine, phenylbutylamine, methylamine and ethylamine , putrescine and spermine. In figure 5, it shows a similar pattern on the activity change from mutation on A156D, F247N, A156D/F427N. Hence, Mutation of A156D and F427N may affect the catalytic activity of AGHO.

When A156 was mutated to polar aspartic acid and F427 was mutated to asparagine at the same time, it may alter the shape of the active site, and aromatic amines with longer chains could not fit into the active site.



#### ***4-2-2. Kinetic studies of A156D, F427N and A156D/F427N mutants with various substrates***

Table 7 shows the kinetic parameters of A156D, F427N and A156D/F427N mutant. Compared with wild type AGHO, the  $K_m$  values of A156D to histamine, benzylamine, phenylethylamine and tyramine increased, but the reactivities of methylamine, ethylamine, phenylpropylamine, phenylbutylamine, putrescine and spermine were too low for the kinetic constants determination.

The  $k_{cat}$  values for the above amine were decreased in A156D. Hence, the  $k_{cat}/K_m$  values for histamine, benzylamine, phenylethylamine and tyramine, were 0.0045, 0.0007, 0.0153 and 0.0112 ( $\mu\text{M}^{-1}\text{S}^{-1}$ ), respectively, which were much

lower than those values of the wild type AGHO. Different from wild type AGHO, no substrate inhibition was observed in this set of mutants including A156D, F427N and A156D/F427N. It was shown that the biogenesis of TPQ of this mutant was unaltered. Thus, A156 of AGHO may play a key role in mediating the catalysis of amines.

The  $K_m$  values of F427N to histamine decreased about 50%. And the  $K_m$  values of F427N to benzylamine, phenylethylamine, phenylpropylamine and tyramine slightly decreased or remained close. The  $k_{cat}$  values for the above amine were decreased.

The  $K_m$  value of A156D/F427N towards histamine is 3 times more than it of the wild type AGHO, to phenylethylamine it is 24 times, and to tyramine it is 10 times. The mutations did change the specificity of these amines. A156D/F427N shows higher reactivities to histamine, phenylethylamine and tyramine but shows no activity to benzylamine. The result shows that the mutation on A156 to aspartic acid and on F427 to asparagine may change the shape or size of the active channel of AGHO, and improve the selectivity on the chain length of these substrates.

### ***4-3. A156S/P157G and L158D mutants***

#### ***4-3-1. Relative activities of A156S/P157G, and L158D mutants with various substrates***

Compared with the wild type AGHO, A156S/P157G exhibits lower



activities to histamine (from 100.0 % to 60.6 %), phenylethylamine (from 145.6 % to 97.6 %) and tyramine (from 112.7 % to 84.8 %), and a slightly increased activity to phenylbutylamine (from 54.2 % to 60.5 %) (Table 8) .Additionally, A156S/P157G shows a relatively low activity to benzylamine (1.1 %). Interesting, the activity of A156S/P157G mutant toward putrescine is higher than that of wild-type (from 0.9% to 1.3%).

L158D mutant exhibited low activity to most of the amines we tested, including histamine (6.3%), benzylamine (1.4 %), phenylethylamine (12.3 %), phenylpropylamine (1.6 %), phenylbutylamine (14.8%) and tyramine (11.9 %). We noticed that the activities toward histamine, phenylethylamine and tyramine decreased more than 10 times of the wild type AGHO. But the activities to aliphatic amines, including putrescine (3.4 %) and spermine (0.9 %) are increased. The result shows that the mutation of L158 to aspartic acid did increase the AGHO activities to the substrates of BSAO and it confirms the result of the previous study made by Chen [16].

#### ***4-3-2. Kinetic studies of A156S/P157G and L158D mutant with various substrates***

Table 9 displays the calculated kinetic constants of A156S/P157G and L158D mutants of AGHO to various substrates.

The previously observed substrate inhibition in wild type by phenylethylamine, phenylpropylamine, phenylbutylamine and tyramine was not

observed in A156S/P157G mutant. The  $K_m$  values for histamine ( $98.58 \pm 1.66 \mu\text{M}$ ), benzylamine ( $91.02 \pm 15.69 \mu\text{M}$ ) and phenylethylamine ( $14.04 \pm 0.13 \mu\text{M}$ ) were higher than those of wild type AGHO. The  $k_{\text{cat}}/K_m$  values of A156S/P157G mutant for histamine, benzylamine, phenylethylamine, tyramine and putrescine were lower than that of wild type AGHO and calculated as 0.0499, 0.0010, 0.3255, 0.3541 and 0.0606 ( $\mu\text{M}^{-1}\text{S}^{-1}$ ), respectively. These results reveal that replacement of A156 to Serine and P157 to Glycine could induce the activity to putrescine. Hence, L158 may be important in determining the substrate selectivity of CAOs. However, A156 and P157 in AGHO may somewhat play roles mediating the substrate selectivity of the enzyme.

For the L158D mutant, the  $K_m$  for histamine ( $148.15 \pm 0.62 \mu\text{M}$ ), phenylethylamine ( $4.64 \pm 0.63 \mu\text{M}$ ) and tyramine ( $12.08 \pm 1.16 \mu\text{M}$ ) was slightly increased or decreased due to the mutation; whereas the  $K_m$  for benzylamine ( $3.6 \pm 2.24 \mu\text{M}$ ) decreased to about 1/10 of wild-type AGHO (Table 9). For the aliphatic amines, including putrescine and spermine, the  $K_m$  values were  $12.86 \pm 1.23 \mu\text{M}$  and  $9.78 \pm 1.92 \mu\text{M}$ , which were too low to be determined in the wild type AGHO. Several amines also exhibit substrate inhibition to L158D mutant, including benzylamine ( $K_i = 606 \pm 270 \mu\text{M}$ ), phenylethylamine ( $K_i = 1401 \pm 250 \mu\text{M}$ ), and tyramine ( $K_i = 1199 \pm 201 \mu\text{M}$ ). Hence, the single mutation of L158D also contributes to mediate the substrate binding and orientation in the active pocket.

L158D and A156S/P157G mutants utilize putrescine and spermine as

substrates. Due to the replacement from Proline to Glycine, the lack of  $\beta$ -carbon atom may permit a substantially greater degree of conformational flexibility and attainable conformational space to admit long chains of amine. As for L158D, it's probably consistent with electrostatic attraction of positively charged substrates into the channel. Therefore it drives the long chains and positively charged amino groups of the substrate to the active site in a correct orientation for the catalytic reaction (Figure 6). This result suggests that A156, P157 and L158 are essential in the active site of AGHO to mediate the substrate recognition and binding.

#### ***4-4. A156S/P157G/L158D, F427S and A156S/P157G/L158D/F427S mutants***

##### ***4-4-1. Relative activities of A156S/P157G/L158D, F427S and***

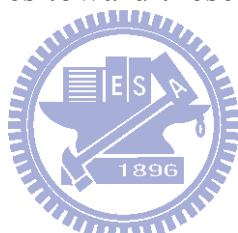
##### ***A156S/P157G/L158D/F427S mutants with various substrates***

Table 10 shows that A156S/P157G/L158D, F427S and A156S/P157G/L158D/F427S mutants all made increased activities to benzylamine, putrescine, and spermine. And they exhibit lower activities to histamine, phenylethylamine, phenylpropylamine, phenylbutylamine and tyramine. The quadruple A156S/P157G/L158D/F427S mutant shows the lowest activities to these amines.

The A156S/P157G/L158D triple mutant shows decreased activities toward histamine (from 100.0% to 9.8%) and phenylethylamine (from 145.6% to 13.3%) to about 1/10 of the wild type AGHO. The A156S/P157G/L158D/F427S

quadruple mutant shows a relatively lower activity toward phenylpropylamine ( $1.4 \pm 0.1\%$ ) which is 1/27 of the wild type AGHO ( $38.1 \pm 1.9\%$ ).

In the F427S mutant the activities toward benzylamine (from 1.8% to 4.0%), putrescine (from 0.9% to 1.9%), and spermine (from 0.4% to 0.8%) were about 2 times for it of the wild type AGHO. In the A156S/P157G/L158D triple mutant the activities toward putrescine ( $6.3 \pm 1.2\%$ ) is 7 times for it of the wild type AGHO ( $0.9 \pm 0.1\%$ ) and for spermine ( $5.6 \pm 0.2\%$ ) it is 14 times for it of the wild type AGHO ( $0.4 \pm 0.1\%$ ). In the A156S/P157G/L158D/F427S quadruple mutant, the activities were even higher. It shows that the mutation on F427 to Serine could enhance the activities toward these aliphatic amines which were typical substrate of BSAO.



#### **4-4-2 Kinetic studies of *A156S/P157G/L158D, F427S and***

##### ***A156S/P157G/L158D/F427S mutants with various substrates***

The calculated kinetic constants of A156S/P157G/L158D, F427S and A156S/P157G/L158D/F427S mutants of AGHO to various substrates are listed in table 11.

A156S/P157G/L158D, F427S and A156S/P157G/L158D/F427S mutant shows similar  $K_m$  values to phenylethylamine, phenylpropylamine, phenylbutylamine and tyramine with the wild type AGHO.  $K_m$  values to histamine and benzylamine were reduced. Interestingly, A156S/P157G/L158D and A156S/P157G/L158D/F427S exhibit higher affinity to putrescine and

spermine with  $K_m$  values larger than 20  $\mu\text{M}$ . And the values are close to the  $K_m$  of BSAO to spermine (20  $\mu\text{M}$ ) [19]. Substrate inhibition was also observed in A156S/P157G/L158D , F427S and A156S/P157G/L158D/F427S mutants. The replacement of these residues with the active site sequence in BASO alters the substrate preference of AGHO from aromatic amine to aliphatic diamines, including putrescine and spermine.

## 5. Conclusion

Phe427 is located near the bottom of the active pocket of AGHO which is close to TPQ402; hence, the mutation on Phe427 into different amino acids could alter the binding of substrates. And the result of this study shows that mutation of Phe427 may change the substrate preference to substrates with specific chain lengths, or change the preferred substrates from aromatic amines to aliphatic amines. It may play an important role in substrate selection due to it locates in the active site, in cooperation with the residues more close to the entry of the channel, we proposed a model of the mutated residues in the active pocket (figure 7) to explain the findings.

## 6. Future Application of AGHO

In the accumulated work, we've found the preferred substrates and kinetics behavior of AGHO. The site-directed mutagenesis study on recombinant AGHO to alter the substrate preference helps to understand how the structure and

residue characteristics affect the substrate specificity on the active site. The activities and kinetics results may be applied into amine detection in the future.

CAOs were found to be potential targets for anti-inflammatory drug screening. The inhibitors of CAOs maybe applied into diabetes treatments. The substrate binding studies in cooperation with drug screening model like GEM-QSAR and GEMDOCK may be useful for more research on proteins characteristics and drug development [27].

The recombinant AGHO and its mutants may be applied to bioselective amine biosensors for the detections of putrescine and cadaverine, which are indicators of the freshness of fish and meat products. Detection method for dopamine may be a possible application to monitor the response of nerve model cells at real time [28, 29].



A study on BSAO-catalyzed oxidation of spermine demonstrated that multidrugresistant (MDR) cancer cells (colon adenocarcinoma and melanoma) are significantly more sensitive than the corresponding wild-type (WT) ones to H<sub>2</sub>O<sub>2</sub> and aldehydes, the products of BSAO-catalyzed oxidation of spermine [30]. And the combination BSAO/spermine prevents tumor growth, particularly. And it is conceivable that combined treatment with a lysosomotropic compound and BSAO/spermine would be effective against tumor cells. The recombinant AGHO mutants that mimic the substrate specificity of BSAO which could be produced and purified efficiently may have the similar application in cancer therapy in the future.

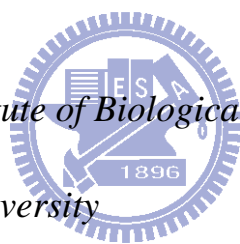
## Reference

1. Samuels, N. M., and Klinman, J. P. (2005) *Biochemistry* **44**, 14308-14317
2. Klinman, J. P. (2003) *Biochim. Biophys. Acta* **1647**, 131-137
3. Cona, A., Rea, G., Angelini, R., Federico, R., and Tavladoraki, P. (2006) *Trends Plant Sci.* **11**, 80-88
4. Brazeau, B. J., Johnson, B. J., and Wilmot, C. M. (2004) *Arch. Biochem. Biophys.* **428**, 22-31
5. Wang, S. X., Nakamura, N., Mure, M., Klinman, J. P., and Sanders-Loehr, J. (1997) *J. Biol. Chem.*, 28841-28844
6. Kumar, V., Dooley, D. M., Freeman, H. C., Guss, J. M., Harvey, I., McGuirl, M. A., Wilce, M. C. J., and Zubak, V. M. (1996) *Structure* **4**, 943-955
7. Parsons, M. R., Convery, M. A., Wilmot, C. M., Yadav, K. D. S., Blakeley, V., Corner, A. S., Phillips, S. E. V., McPherson, M. J., and Knowles, P. F. (1995) *Structure* **3**, 1171-1184
8. Wilce, M. C. J., Dooley, D. M., Freeman, H. C., Guss, J. M., Matsunami, H., McIntire, W. S., Ruggiero, C. E., Tanizawa, K., and Yamaguchi, H. (1997) *Biochemistry* **36**, 16116-16133
9. Li, R., Chen, L., Cai, D., Klinman, J. P., and Mathews, F. S. (1997) *Acta*

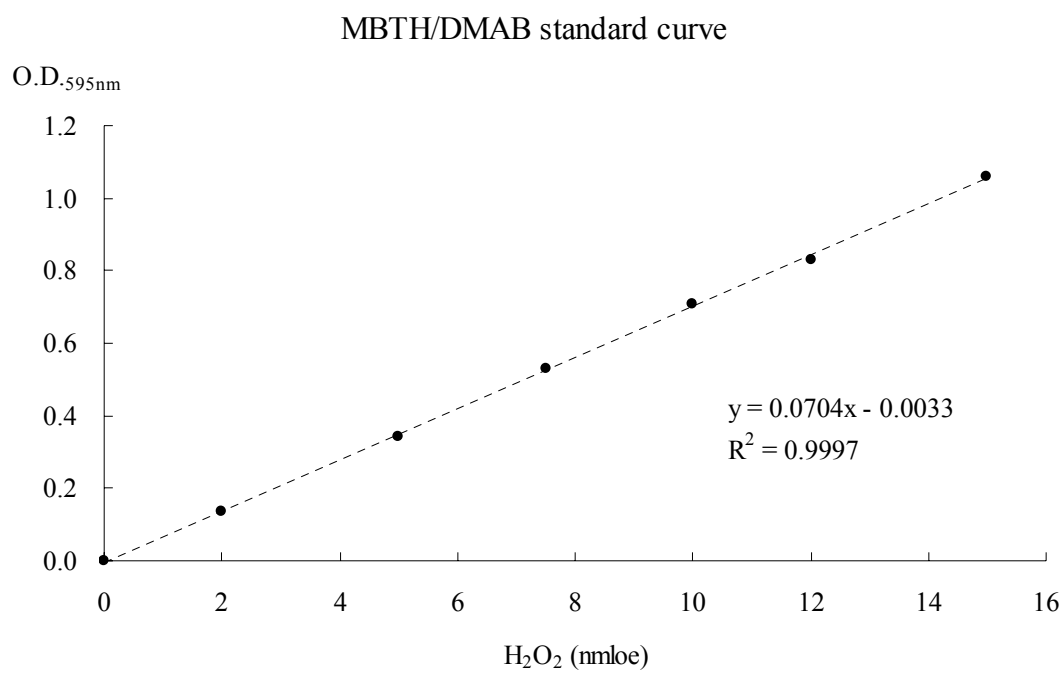
- Crystallogr., Sect. D: Biol. Crystallogr.* **53**, 364-370
10. Lunelli, M., Paolo, M. L. D., Biadene, M., Calderone, V., Battistutta, R., Scarpa, M., Rigo, A., and Zanotti, G. (2005) *J. Mol. Biol.* **346**, 991-1004
  11. Airene, T. T., Nymalm, Y., Kidron, H., Smith, D. J., Pihlavisto, M., Salmi, M., Jalkanen, S., Johnson, M. S., and Salminen, T. A. (2005) *Protein Sci.* **14**, 1964-1974
  12. Duff, A. P., Cohen, A. E., Ellis, P. J., Kuchar, J. A., Langley, D. B., Shepard, E. M., Dooley, D. M., Freeman, H. C., and Guss, J. M. (2003) *Biochemistry* **42**, 15148-15157
  13. Matsuzaki, R., and Tanizawa, K. (1998) *Biochemistry* **37**, 13947-13957
  14. Wilmot, C. M., Murray, J. M., Alton, G., Parsons, M. R., Convery, M. A., Blakeley, V., Corner, A. S., Palcic, M. M., Knowles, P. F., McPherson, M. J., and Phillips, S. E. V. (1997) *Biochemistry* **36**, 1608-1620
  15. Yang, J.-G. (2004) *Institute of Biological Science and Technology, National Chiao Tung University*
  16. Chen, S.-Y. (2006) *Institute of Biological Science and Technology, National Chiao Tung University*
  17. Murray, J. M., Kurtis, C. R., Tambyrajah, W., Saysell, C. G., Wilmot, C. M., Parsons, M. R., Phillips, S. E. V., Knowles, P. F., and McPherson, M.



- J. (2001) *Biochemistry* **40**, 12808-12818
18. Houen, G., Struve, C., Søndergaard, R., Friis, T., Anthoni, U., Nielsen, P. H., Christophersen, C., Petersen, B. O., and Duus, J. Ø. (2005) *Bioorg. Med. Chem.* **13**, 3783-3796
19. Paolo, M. L. D., Stevanato, R., Corazza, A., Vianello, F., Lunelli, L., Scarpa, M., and Rigo, A. (2003) *Biochem. J.* **371**, 549-556
20. Lee, Y., and Sayre, L. M. (1998) *J. Biol. Chem.* **273**, 19490-19494
21. Chang, L.-J. (2005) *Institute of Bioinformatics, National Chiao Tung University*
22. Chang, S.-P. (2003) *Institute of Biological Science and Technology, National Chiao Tung University*
23. Lin, Y.-H. (2002) *Institute of Biological Science and Technology, National Chiao Tung University*
24. Stoner, P. (1985) *Agents Actions* **17**, 5-9
25. Paz, M. A., Fliickiger, R., Boak, A., Kagan, H. M., and Gallop, P. M. (1991) *J. Biol. Chem.* **266**, 689-692
26. Shimizu, E., Odawara, T., Tanizawa, K., and Yorifuji, T. (1994) *Biosci., Biotechnol., Biochem.* **58**, 2118-2120
27. Marti, L., Abella, A., Cruz, X. d. l., García-Vicente, S., Unzeta, M.,

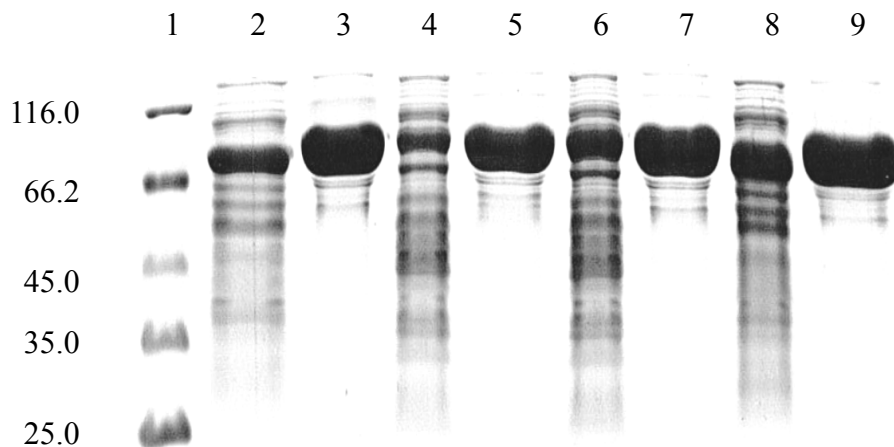


- Carpéné, C., Palacín, M., Testar, X., Orozco, M., and Zorzano, A. (2004)  
*J. Med. Chem.* **47**, 4865-4874
28. Shinohara, H., and Wang, F. (2007) *Anal. Sci.* **23**, 81-84
29. Lizcano, J. M., Balsa, D., Tipton, K. F., and Unzeta, M. (1991) *Biochem. Pharmacol.* **41**, 1107–1110
30. Agostinelli, E., Tempera, G., Viceconte, N., Saccoccio, S., Battaglia, V., Grancara, S., Toninello, A., and Stevanato, R. (2009) *Amino Acids*  
**(Published online: 10 December 2009)**
31. Li, R., Klinman, J. P., and Mathews, F. S. (1998) *Structure* **6**, 293-307
32. Cai, D., and Klinman, J. P. (1994) *Biochemistry* **33**, 7647-7653
33. Tipping, A. J., and McPherson, M. J. (1995) *J. Biol. Chem.* **270**,  
16939-16946



**Figure 1.** The H<sub>2</sub>O<sub>2</sub> standard curve was determined within the range from 0.1 to 15 nmole of H<sub>2</sub>O<sub>2</sub>.





**Figure 2.** 10% SDS-PAGE of crude extract and purified protein of wild type AGHO and its mutants. Relative intensities of purified proteins were analyzed and calculated by ImageJ software.

Lane1: molecular weight standards (MBI marker)

Lane2: crude extract of wild type AGHO

Lane3: purified wild type AGHO (relative intensity of the major band is 0.9949)

Lane4: crude extract of A156D

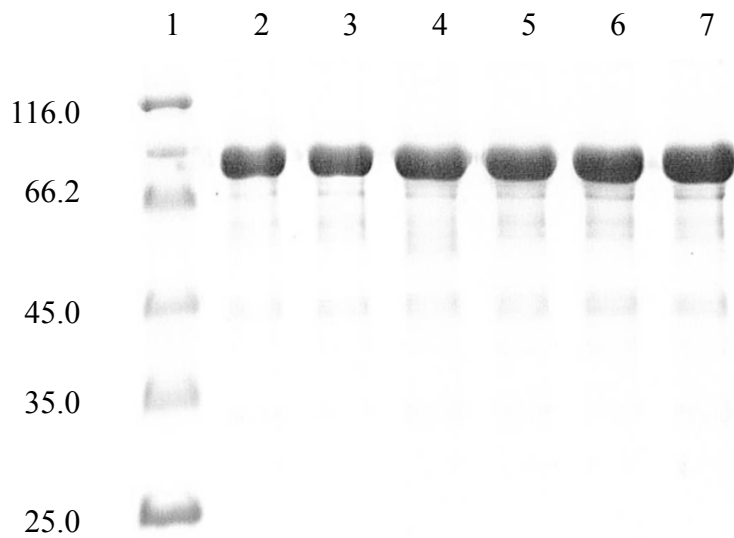
Lane5: purified A156D (relative intensity of the major band is 0.9912)

Lane6: crude extract of F427N

Lane7: purified F427N (relative intensity of the major band is 0.9983)

Lane8: crude extract of A156D/F427N

Lane9: purified A156D/F427N (relative intensity of the major band is 0.9870)



**Figure 3.** 10% SDS-PAGE of purified of wild type AGHO and its mutants.

Relative intensities of purified proteins were analyzed and calculated by ImageJ software.

Lane1: molecular weight standards (MBI marker)

Lane2: purified wild type AGHO (relative intensity of the major band is 0.9974)

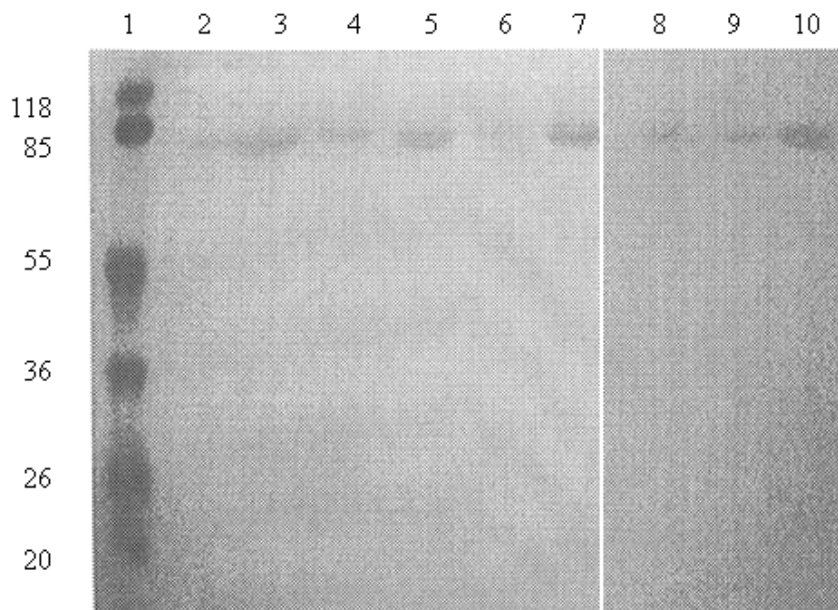
Lane3: purified A156S/P157G/L158D (relative intensity of the major band is 0.9981)

Lane4: purified F427S (relative intensity of the major band is 0.9968)

Lane5: purified A156S/P157G/L158D/F427S (relative intensity of the major band is 0.9909)

Lane6: purified L158D (relative intensity of the major band is 0.9850)

Lane7: purified A156S/P157G (relative intensity of the major band is 0.9858)



**Figure 4.** NBT/glycinate staining of the wild type AGHO and the its mutants.

Lane1: molecular weight marker

Lane2: purified wild type AGHO containing Cu<sup>2+</sup>

Lane3: purified A156D containing Cu<sup>2+</sup>

Lane4: purified F427N containing Cu<sup>2+</sup>

Lane5: purified A156D/F427N containing Cu<sup>2+</sup>

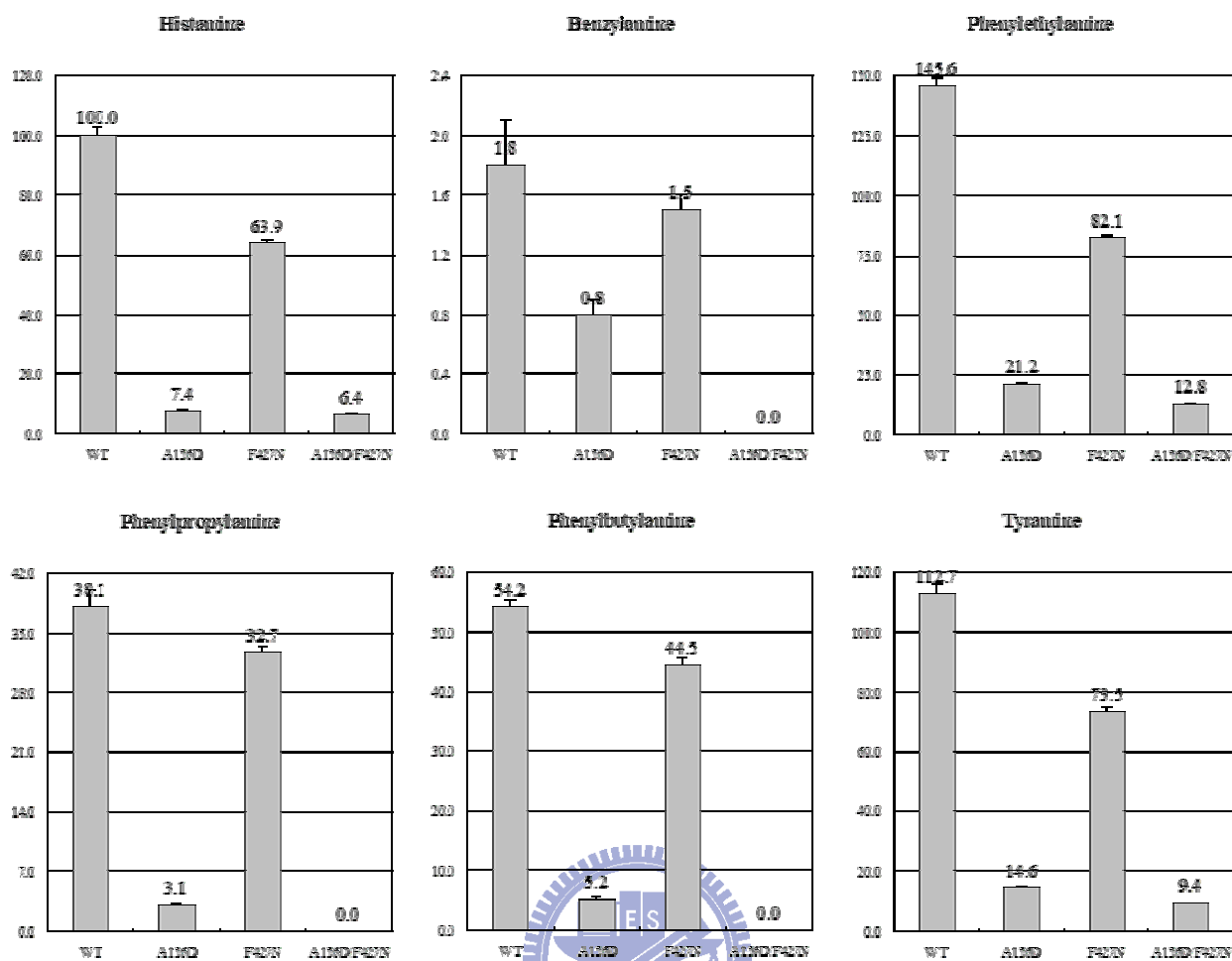
Lane6: purified A156S/P157G containing Cu<sup>2+</sup>

Lane7: purified L158D containing Cu<sup>2+</sup>

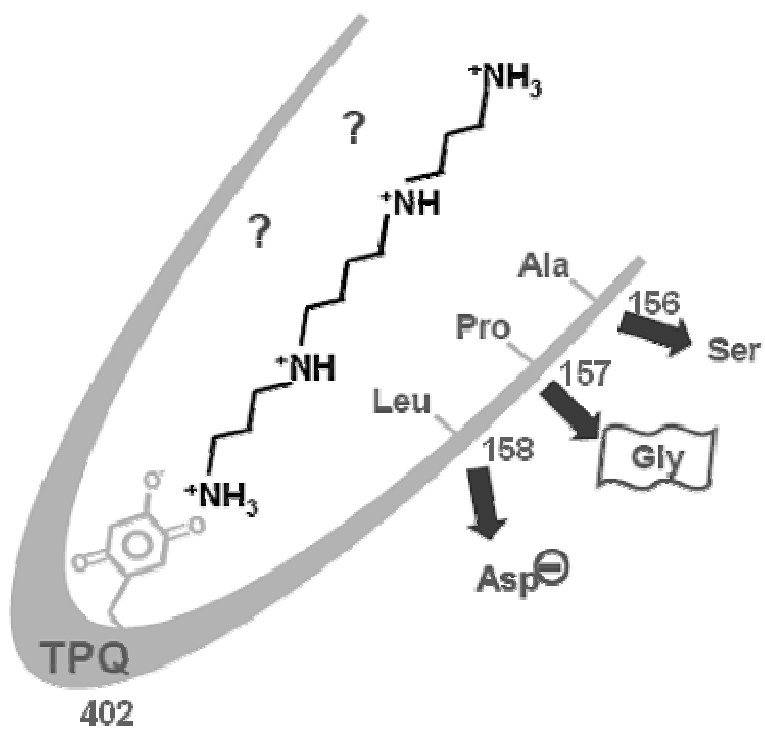
Lane8: purified A156S/P157G/L158D containing Cu<sup>2+</sup>

Lane9: purified F427S containing Cu<sup>2+</sup>

Lane10: purified A156S/P157G/L158D/F427S containing Cu<sup>2+</sup>



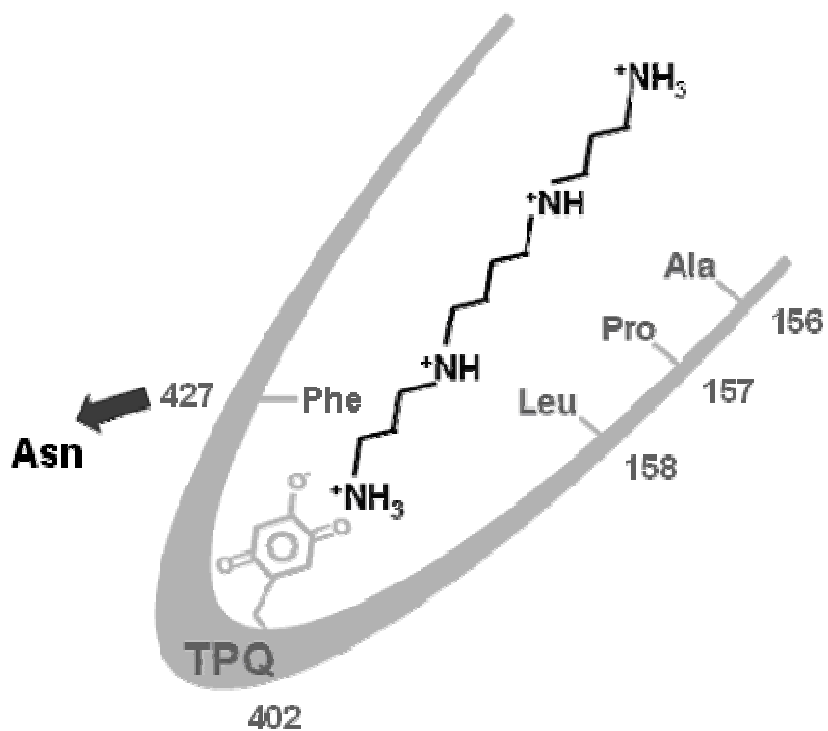
**Figure 5.** Plots of relative activities toward various amines between wild type AGHO and A156D, F427N and 156D/F427N.



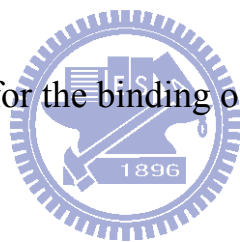
**Figure 6.** The proposed model for the binding of spermine in the active site of A156S/P157G/L158D.







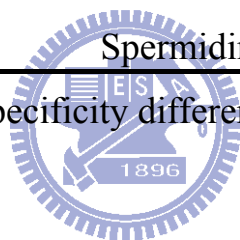
**Figure 7.** The proposed model for the binding of spermine in the active site of A156, P157, L158 and F427.



**Table 1.** CAOs are known to vary a great deal in their preferred substrate specificities.

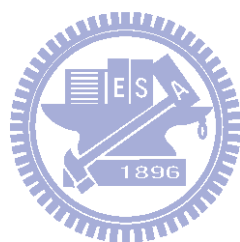
<b>The Source of Amine oxidase</b>	<b>Preferred Substrates</b>
Kingdom Monera	<u>Aromatic amines</u>
e.g. AGPEO [8], ECAO[16]	Phenylethylamine, Tyramine...
Kingdom Fungi	<u>Small aliphatic amines</u>
e.g. HPAO [31, 32]	Methylamine, Ethylamine...
Kingdom Plantae	<u>Diamines</u>
e.g. PSAO [33]	Putrescine, Cadaverine...
Kingdom Animalia	<u>Long chains and hydrophobic character of amines</u>
e.g. BSAO [18,19,20]	Spermidine, Spermine...

CAOs exhibit broad substrate specificity differences depending on different sources.



**Table 2.** Relative activities of wild type AGHO reacted with various substrates.

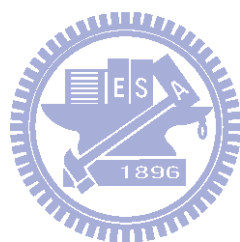
<b>Substrate</b>	<b>Relative activities (%)</b>
Histamine	100.0 ± 3.0
Benzylamine	1.8 ± 0.3
Phenylethylamine	145.6 ± 3.6
Phenylpropylamine	38.1 ± 1.9
Phenylbutylamine	54.2 ± 1.3
Tyramine	112.7 ± 3.2
Putrescine	0.9 ± 0.1
Spermine	0.4 ± 0.1



**Table 3.**  $K_m$ ,  $K_{cat}$ ,  $K_i$  and  $K_{cat} / K_m$  values toward various substrates of wild type AGHO.

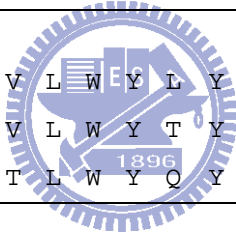
WT	$K_m$ ( $\mu\text{M}$ )	$K_{cat}$ ( $\text{S}^{-1}$ )	$K_i$ ( $\mu\text{M}$ )	$K_{cat} / K_m$ ( $\mu\text{M}^{-1} \text{S}^{-1}$ )
Histamine	83.92 $\pm$ 2.70	7.51 $\pm$ 0.09	—	0.0895
Benzylamine	49.01 $\pm$ 12.03	0.11 $\pm$ 0.01	—	0.0220
Phenylethylamine	9.05 $\pm$ 0.45	7.63 $\pm$ 0.11	544 $\pm$ 28	0.8431
Phenylpropylamine	7.50 $\pm$ 0.97	2.17 $\pm$ 0.08	330 $\pm$ 35	0.2889
Phenylbutylamine	2.23 $\pm$ 0.60	2.78 $\pm$ 0.10	428 $\pm$ 53	1.2484
Tyramine	12.37 $\pm$ 0.66	5.70 $\pm$ 0.10	870 $\pm$ 67	0.4606
Putrescine	— <sup>a</sup>	—	—	—
Spermine	—	—	—	—

<sup>a</sup>The negative symbol (—) denotes that the reaction rate was too slow to determine.



**Table 4.** The multiple sequences alignment of residues of the channel from different CAOs.

Residue number	123	124	126	127	130	154	156	157	158	177	181	189	304	313	316	318	322	327	377	378	379	398	399	400	401	402	427
<b>Kingdom Monera</b>																											
AGHO	L	E	F	G	E	R	A	P	L	L	Q	W	Y	W	Y	D	Y	D	D	E	W	T	V	G	N	Y	F
AGPEO	E	E	F	E	E	R	A	P	L	L	Q	W	Y	W	Y	D	Y	Y	D	L	W	T	I	G	N	Y	F
ECAO	L	D	F	A	Q	I	T	P	L	I	D	W	Y	F	Y	D	Y	L	E	M	G	T	V	G	N	Y	A
KAMO	L	D	F	V	Q	V	T	P	L	V	D	W	Y	F	Y	D	Y	L	E	M	G	T	V	G	N	Y	A
<b>Kingdom Fungi</b>																											
ASNAO	L	T	S	E	T	V	E	P	W	L	T	Y	Y	R	A	D	G	M	N	W	R	T	L	A	N	Y	N
HPAO	V	E	L	C	E	Y	D	P	W	L	R	Y	Y	R	A	D	Y	M	D	F	R	T	A	A	N	Y	N
<b>Kingdom Plantae</b>																											
LSAO	S	A	E	Q	A	V	S	S	F	D	K	Y	Y	F	F	D	F	S	E	T	G	T	V	G	N	Y	E
PSAO	S	V	E	Q	A	V	S	S	F	D	K	Y	Y	F	F	D	F	S	E	N	G	T	V	G	N	Y	E
<b>Kingdom Animalia</b>																											
BSAO	L	R	Y	L	D	V	S	G	D	V	L	W	Y	L	Y	D	F	F	H	S	D	T	M	L	N	Y	S
hVAP-1	F	Q	Y	L	D	L	S	G	D	V	L	W	Y	T	Y	D	F	Y	H	S	D	T	L	L	N	Y	S
hABP	T	A	Y	A	Y	V	S	G	Q	T	L	W	Y	Q	Y	D	W	V	F	N	S	T	V	Y	N	Y	H



**Table 5.** The multiple sequences alignment of CAOs on the selected residues involved in substrate binding.

Number of Amino Acids Involve in Substrate Binding										
Residue number	126	156	157	158	316	318	322	399	401	427
AGHO	F	A	P	L	Y	D	Y	V	N	F
AGPEO	F	A	P	L	Y	D	Y	I	N	F
ECAO	F	T	P	L	Y	D	Y	V	N	A
KAMO	F	T	P	L	Y	D	Y	V	N	A
ASNAO	S	E	P	W	A	D	G	L	N	N
HPAO	L	D	P	W	A	D	Y	A	N	N
LSAO		S	S	F	F	D	F	V	N	E
PSAO	E	S	S	F	F	D	F	V	N	E
BSAO	Y	S	G	D	Y	D	F	M	N	S
hVAP-1	Y	S	G	D	Y	D	F	L	N	S
hABP	Y	S	G	Q	Y	D	W	V	N	H

The residue number showed in table is derived from the sequence of AGHO.

**Table 6.** Relative activities of A156D, F427N and A156D/F427N mutants of AGHO reacted with various substrates.

<b>Substrate</b>	<b>WT</b>	<b>A156D</b>	<b>F427N</b>	<b>A156D/F427N</b>
Histamine	100.0 ± 3.0	7.4 ± 0.2	63.9 ± 1.0	6.4 ± 0.2
Benzylamine	1.8 ± 0.3	0.8 ± 0.1	1.5 ± 0.1	—
Phenylethylamine	145.6 ± 3.6	21.2 ± 0.3	82.1 ± 1.6	12.8 ± 0.2
Phenylpropylamine	38.1 ± 1.9	3.1 ± 0.2	32.7 ± 0.8	—
Phenylbutylamine	54.2 ± 1.3	5.2 ± 0.5	44.5 ± 1.2	—
Tyramine	112.7 ± 3.2	14.6 ± 0.3	73.5 ± 1.8	9.4 ± 0.2
Methylamine	—	—	—	—
Ethylamine	—	—	—	—
Putrescine	0.9 ± 0.1	—	—	—
Spermine	0.4 ± 0.1	—	—	—



**Table 7.**  $K_m$ ,  $K_{cat}$ ,  $K_i$  and  $K_{cat} / K_m$  values toward various substrates of A156D (A), F427N (B) and A156D/F427N (C) mutants of AGHO

(A)

<b>A156D</b>	$K_m$ ( $\mu\text{M}$ )	$K_{cat}$ ( $\text{S}^{-1}$ )	$K_i$ ( $\mu\text{M}$ )	$K_{cat} / K_m$ ( $\mu\text{M}^{-1} \text{S}^{-1}$ )
Histamine	201.40 $\pm$ 6.32	0.91 $\pm$ 0.01	—	0.0045
Benzylamine	105.11 $\pm$ 19.69	0.07 $\pm$ 0.01	—	0.0007
Phenylethylamine	134.47 $\pm$ 5.38	2.05 $\pm$ 0.03	—	0.0153
Phenylpropylamine	—	—	—	—
Phenylbutylamine	—	—	—	—
Tyramine	114.34 $\pm$ 5.46	1.28 $\pm$ 0.02	—	0.0112
Putrescine	—	—	—	—
Spermine	—	—	—	—

(B)

<b>F427N</b>	$K_m$ ( $\mu\text{M}$ )	$K_{cat}$ ( $\text{S}^{-1}$ )	$K_i$ ( $\mu\text{M}$ )	$K_{cat} / K_m$ ( $\mu\text{M}^{-1} \text{S}^{-1}$ )
Histamine	36.49 $\pm$ 0.89	3.60 $\pm$ 0.02	—	0.0985
Benzylamine	30.12 $\pm$ 3.32	0.08 $\pm$ 0.002	—	0.0027
Phenylethylamine	8.34 $\pm$ 0.32	3.63 $\pm$ 0.02	—	0.4348
Phenylpropylamine	4.21 $\pm$ 0.31	1.40 $\pm$ 0.01	—	0.3334
Phenylbutylamine	2.92 $\pm$ 0.23	1.88 $\pm$ 0.01	—	0.6454
Tyramine	8.66 $\pm$ 0.24	3.28 $\pm$ 0.02	—	0.3787
Putrescine	—	—	—	—
Spermine	—	—	—	—



**Table 7. Continued**

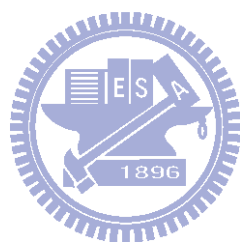
(C)

<b>A156D/F427N</b>	$K_m$ ( $\mu\text{M}$ )	$K_{cat}$ ( $\text{S}^{-1}$ )	$K_i$ ( $\mu\text{M}$ )	$K_{cat}/K_m$ ( $\mu\text{M}^{-1} \text{S}^{-1}$ )
Histamine	249.09 $\pm$ 7.94	0.91 $\pm$ 0.02	—	0.0037
Benzylamine	—	—	—	—
Phenylethylamine	220.96 $\pm$ 9.68	1.69 $\pm$ 0.04	—	0.0076
Phenylpropylamine	—	—	—	—
Phenylbutylamine	—	—	—	—
Tyramine	125.30 $\pm$ 5.15	0.86 $\pm$ 0.01	—	0.0069
Putrescine	—	—	—	—
Spermine	—	—	—	—



**Table 8.** Relative activities of L158D and A156S/P157G mutants of AGHO reacted with various substrates.

<b>Substrate</b>	<b>WT</b>	<b>L158D</b>	<b>A156S/P157G</b>
Histamine	100.0 ± 3.0	6.3 ± 1.6	60.6 ± 0.7
Benzylamine	1.8 ± 0.3	1.4 ± 0.2	1.1 ± 0.2
Phenylethylamine	145.6 ± 3.6	12.3 ± 0.2	97.6 ± 0.8
Phenylpropylamine	38.1 ± 1.9	1.6 ± 0.1	26.6 ± 0.6
Phenylbutylamine	54.2 ± 1.3	14.8 ± 0.2	60.5 ± 1.0
Tyramine	112.7 ± 3.2	11.9 ± 0.3	84.8 ± 0.3
Putrescine	0.9 ± 0.1	3.4 ± 0.3	1.3 ± 0.3
Spermine	0.4 ± 0.1	0.9 ± 0.2	—



**Table 9.**  $K_m$ ,  $K_{cat}$ ,  $K_i$  and  $K_{cat} / K_m$  values toward various substrates of L158D (A) and A156S/P157G (B) mutants of AGHO

(A)

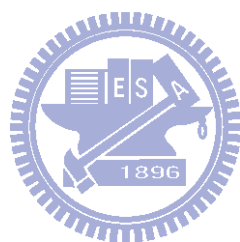
<b>L158D</b>	$K_m$ ( $\mu\text{M}$ )	$K_{cat}$ ( $\text{S}^{-1}$ )	$K_i$ ( $\mu\text{M}$ )	$K_{cat} / K_m$ ( $\mu\text{M}^{-1} \text{S}^{-1}$ )
Histamine	148.15 $\pm$ 0.62	0.47 $\pm$ 0.09	—	0.0032
Benzylamine	3.60 $\pm$ 2.24	0.07 $\pm$ 0.01	606 $\pm$ 270	0.0194
Phenylethylamine	4.64 $\pm$ 0.63	0.56 $\pm$ 0.01	1401 $\pm$ 250	0.1207
Phenylpropylamine	—	—	—	—
Phenylbutylamine	—	—	—	—
Tyramine	12.08 $\pm$ 1.16	0.60 $\pm$ 0.02	1199 $\pm$ 201	0.0497
Putrescine	12.86 $\pm$ 1.23	0.32 $\pm$ 0.01	—	0.0025
Spermine	9.78 $\pm$ 1.92	0.41 $\pm$ 0.06	—	0.0042

(B)

<b>A156S/P157G</b>	$K_m$ ( $\mu\text{M}$ )	$K_{cat}$ ( $\text{S}^{-1}$ )	$K_i$ ( $\mu\text{M}$ )	$K_{cat} / K_m$ ( $\mu\text{M}^{-1} \text{S}^{-1}$ )
Histamine	98.58 $\pm$ 1.66	4.92 $\pm$ 0.03	—	0.0499
Benzylamine	91.02 $\pm$ 15.69	0.09 $\pm$ 0.005	—	0.0010
Phenylethylamine	14.04 $\pm$ 0.13	4.57 $\pm$ 0.01	—	0.3255
Phenylpropylamine	—	—	—	—
Phenylbutylamine	—	—	—	—
Tyramine	10.93 $\pm$ 0.10	3.87 $\pm$ 0.01	—	0.3541
Putrescine	7.76 $\pm$ 1.47	0.47 $\pm$ 0.06	—	0.0606
Spermine	—	—	—	—

**Table 10.** Relative activities of A156S/P157G/L158D, F427S and A156S/P157G/L158D/F427S mutants of AGHO reacted with various substrates.

Substrate	WT	A156S/P157G/L158D	F427S	A156S/P157G/L158D/F427S
Histamine	100.0 ± 3.0	9.8 ± 1.5	43.8 ± 0.5	18.7 ± 0.4
Benzylamine	1.8 ± 0.3	1.9 ± 0.1	4.0 ± 0.1	2.7 ± 0.3
Phenylethylamine	145.6 ± 3.6	13.3 ± 0.6	44.0 ± 0.6	32.0 ± 0.9
Phenylpropylamine	38.1 ± 1.9	1.9 ± 0.1	19.2 ± 0.4	1.4 ± 0.1
Phenylbutylamine	54.2 ± 1.3	19.9 ± 0.7	22.9 ± 0.1	19.1 ± 0.7
Tyramine	112.7 ± 3.2	15.4 ± 0.6	52.0 ± 0.9	25.2 ± 0.5
Putrescine	0.9 ± 0.1	6.3 ± 1.2	1.9 ± 0.1	8.0 ± 1.0
Spermine	0.4 ± 0.1	5.6 ± 0.2	0.8 ± 0.2	6.9 ± 0.1



**Table 11.**  $K_m$ ,  $K_{cat}$ ,  $K_i$  and  $K_{cat}/K_m$  values toward various substrates of A156S/P157G/L158D (A), F427S (B) and A156S/P157G/L158D/F427S (C) mutants of AGHO.

(A)

<b>A156S/P157G/L158D</b>	$K_m$ ( $\mu\text{M}$ )	$K_{cat}$ ( $\text{S}^{-1}$ )	$K_i$ ( $\mu\text{M}$ )	$K_{cat}/K_m$ ( $\mu\text{M}^{-1} \text{S}^{-1}$ )
Histamine	40.16 $\pm$ 7.00	0.56 $\pm$ 0.03	—	0.0139
Benzylamine	18.00 $\pm$ 1.86	0.09 $\pm$ 0.002	—	0.0050
Phenylethylamine	7.84 $\pm$ 2.47	0.62 $\pm$ 0.05	1626 $\pm$ 952	0.0793
Phenylpropylamine	6.08 $\pm$ 1.37	0.08 $\pm$ 0.003	—	0.0136
Phenylbutylamine	2.70 $\pm$ 0.93	1.08 $\pm$ 0.06	312 $\pm$ 50	0.4015
Tyramine	12.10 $\pm$ 2.29	0.75 $\pm$ 0.04	1659 $\pm$ 686	0.0618
Putrescine	21.35 $\pm$ 3.15	0.31 $\pm$ 0.01	—	0.0145
Spermine	25.08 $\pm$ 2.42	0.29 $\pm$ 0.01	2780 $\pm$ 1022	0.0117

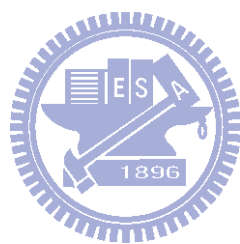
(B)

<b>F427S</b>	$K_m$ ( $\mu\text{M}$ )	$K_{cat}$ ( $\text{S}^{-1}$ )	$K_i$ ( $\mu\text{M}$ )	$K_{cat}/K_m$ ( $\mu\text{M}^{-1} \text{S}^{-1}$ )
Histamine	50.33 $\pm$ 1.57	2.71 $\pm$ 0.03	—	0.0539
Benzylamine	27.02 $\pm$ 1.11	0.21 $\pm$ 0.002	—	0.0078
Phenylethylamine	7.40 $\pm$ 0.43	2.15 $\pm$ 0.03	838 $\pm$ 59	0.2904
Phenylpropylamine	4.91 $\pm$ 0.33	0.96 $\pm$ 0.01	588 $\pm$ 33	0.1959
Phenylbutylamine	1.92 $\pm$ 0.19	1.07 $\pm$ 0.01	809 $\pm$ 42	0.5590
Tyramine	9.37 $\pm$ 0.39	2.54 $\pm$ 0.03	1034 $\pm$ 64	0.2706
Putrescine	1.65 $\pm$ 0.29	0.08 $\pm$ 0.001	—	0.0485
Spermine	—	—	—	—

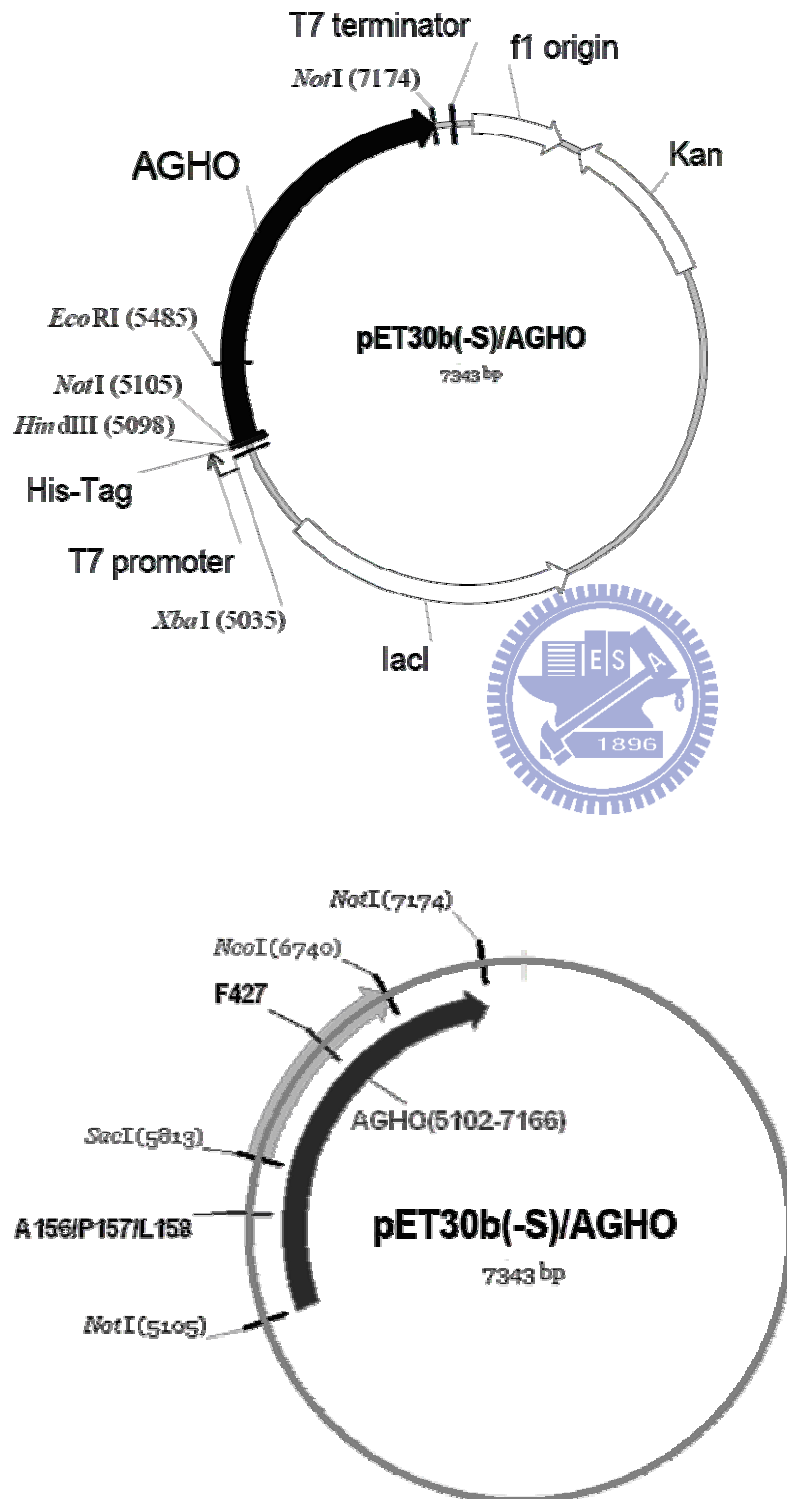
**Table 11.** Continued

(C)

<b>A156S/P157G /L158D/ F427S</b>	$K_m$ ( $\mu\text{M}$ )	$K_{cat}$ ( $\text{S}^{-1}$ )	$K_i$ ( $\mu\text{M}$ )	$K_{cat}/K_m$ ( $\mu\text{M}^{-1} \text{S}^{-1}$ )
Histamine	44.45 $\pm$ 3.77	1.11 $\pm$ 0.03	—	0.0250
Benzylamine	16.74 $\pm$ 1.82	0.13 $\pm$ 0.003	—	0.0078
Phenylethylamine	6.36 $\pm$ 0.42	1.49 $\pm$ 0.02	1394 $\pm$ 140	0.2346
Phenylpropylamine	6.62 $\pm$ 0.80	0.06 $\pm$ 0.001	—	0.0092
Phenylbutylamine	2.78 $\pm$ 0.73	0.96 $\pm$ 0.04	523 $\pm$ 78	0.3445
Tyramine	8.25 $\pm$ 0.80	1.23 $\pm$ 0.03	930 $\pm$ 119	0.1488
Putrescine	24.63 $\pm$ 2.72	0.41 $\pm$ 0.01	—	0.0166
Spermine	26.99 $\pm$ 6.03	0.38 $\pm$ 0.04	1605 $\pm$ 908	0.0141

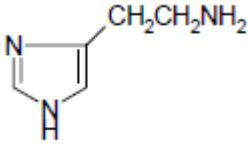
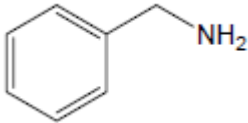
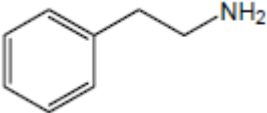
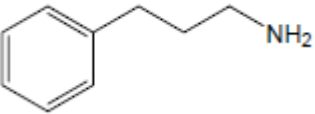
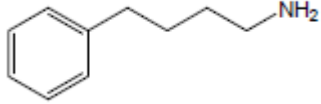
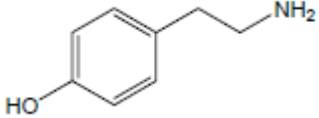


## Appendix 1. Plasmid map of pET30b(-S)/AGHO



## Appendix 2. List of amines

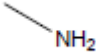

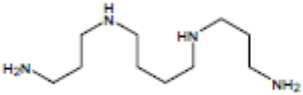

### Aromatic amines:

Chemical name Molecular Formula	Synonyms	Structural formula
Histamine $C_5H_9N_3$	2-(4-Imidazolyl)ethylamine	
Benzylamine $C_7H_9N$		
Phenylethylamine $C_8H_{11}N$		
Phenylpropylamine $C_9H_{13}N$		
Phenylbutylamine $C_{11}H_{13}N$		
Tyramine $C_8H_{11}NO$		



## Appendix 2. Continued

### Aliphatic amines:

Chemical name Molecular Formula	Synonyms	Structural formula
Methylamine $\text{CH}_5\text{N}$	Aminomethane; Methanamine; Monomethylamine	
Ethylamine $\text{C}_2\text{H}_7\text{N}$	Aminoethane; Ethanamine; Monoethylamine	
Spermine $\text{C}_{10}\text{H}_{26}\text{N}_4$	N,N'-Bis(3-aminopropyl)- 1,4-diaminobutane	
1,4-Diaminobutane $\text{C}_4\text{H}_{12}\text{N}_2$	1,4-Butanediamine; Putrescine	



### Appendix 3. List of plasmids and vectors

	Name	Origin
1	pET30(-S)/AGHO	Chang S-. P., 2003
2	pGEM-T easy/AGHO-reverse	Chen S-. Y., 2006
3	pGEM-T easy/AGHO-reverse(A156D)	Chen S-. Y., 2006
4	pGEM-T easy/AGHO-reverse(F427N)	This project
5	pGEM-T easy/AGHO-reverse(A156D/F427N)	This project
6	pGEM-T easy/AGHO-reverse(A156S/P157G)	Chen S-. Y., 2006
7	pGEM-T easy/AGHO-reverse(L158D)	Chen S-. Y., 2006
8	pGEM-T easy/AGHO-reverse(A156S/P157G/L158D)	Chen S-. Y., 2006
9	pGEM-T easy/AGHO-reverse(F427S)	This project
10	pGEM-T easy/AGHO-reverse(A156S/P157G/L158D/F427S)	This project
11	pET30b(-S)/AGHO(A156D)	Chen S-. Y., 2006
12	pET30b(-S)/AGHO(F427N)	This project
13	pET30b(-S)/AGHO(A156D/F427N)	This project
14	pET30b(-S)/AGHO(A156S/P157G)	Chen S-. Y., 2006
15	pET30b(-S)/AGHO(L158D)	Chen S-. Y., 2006
16	pET30b(-S)/AGHO(A156S/P157G/L158D)	Chen S-. Y., 2006
17	pET30b(-S)/AGHO(F427S)	This project
18	pET30b(-S)/AGHO(A156S/P157G/L158D/F427S)	This project

**Appendix 4.** List of primers for site-directed mutagenesis

Primer	Sequence (from the 5' end to the 3' end)
Sequence primer (L)	5'-GCCGGCTGGGACCTGCGC-3'
Sequence primer (R)	5'-CTGTGCCACGTAGGCGGG-3'
F427N (L)	5'-CGGGCATCGTGA <u>AA</u> CACGGCAGCGCTCCC-3'
F427N (R)	5'-GGGAGCGCTGCCGTG <u>TT</u> CACGATGCCCCG-3'
F427S (L)	5'-CGGGCAT <u>CT</u> GTGTCGACGGCAGCGCTCC-3'
F427S (R)	5'-GGAGCGCTGCCGTGACAC <u>GAT</u> GCCCCG-3'



## Appendix 5. Abbreviations of CAOs from different source

AGHO *Arthrobacter globiformis* Histamine Oxidase

AGPEO *Arthrobacter globiformis* Phenylethylamine Oxidase

ECAO *Escherichia coli* Amine Oxidase

KAMO *Klesiellus aerogenes* Monoamine Oxidase

ASNAO *Aspergillus niger* Amine Oxidase

HPAO *Hansenula Polymorpha* metylamine Oxidase

LSAO *Lentil* Seedling Amine Oxidase

PSAO *Pea* Seedling Amine Oxidase

BSAO *Bovine* Serum Amine Oxidase

hVAP-1 *Human* Vascular Adhesion Protein-1

hABP *Human* Amiloride-Binding Protein

